

Fibre-on-plate experiments: relaxation and surface tension

G. DE WITH*, A. J. CORBIJN

Philips Research Laboratories, Prof Holstlaan 4, 5656 AA, Eindhoven, The Netherlands

The relaxation of the fibre-on-plate geometry was studied experimentally using glass. Various fibre diameters and temperature/time schedules were used. Excellent agreement with the theoretical predictions of Hopper was obtained. The determination of the surface tension of glass at low temperature by this method is discussed. A value of 0.19 N m^{-1} at 600°C was measured for a modified Na–K–Ba–Sr–silica glass, which differs significantly from the sessile-drop value of 0.35 N m^{-1} , extrapolated from high-temperature data. Influencing factors are discussed. The difference is probably due to the presence of water vapour which considerably lowers the surface tension of glass at low temperature.

1. Introduction

Relaxation of glass surfaces under the influence of surface tension has been limitedly studied. Some geometrical arrangements were theoretically studied by Hopper [1]. A particularly interesting configuration is the fibre-on-plate geometry. For this geometry, relatively simple expressions are obtained from the complex analysis, which possibly can be applied in further experiments. The first aim of this work was, therefore, to verify experimentally the time-dependent relaxation as described theoretically by Hopper.

The second aim was to apply the results for the determination of the surface tension of glasses. Measurement of the surface tension of glass is also a somewhat neglected area. In contrast to the viscosity, for which a variety of methods covering a wide temperature range is available, methods for measuring surface tension are limited in number. The sessile drop method is conventionally used [2, 3] for high temperatures. In the case of low(er) temperatures, the fibre extension method can, in principle, be used if the measurements are extended over a range of forces in such a way that shrinking as well as extending fibres are encountered. In this paper another method is described which is based on the deforming geometry of a fibre on a plate. As mentioned, for such a fibre, given the viscosity and surface tension, the deformation can be modelled analytically. Hence if one determines the deformed geometry of a fibre, an estimate of the surface tension can be made once the viscosity is known. The background has been highlighted, and the experimental details are given. The results are discussed and a set of conclusions is presented.

2. Theory

The description of relaxing glass surfaces is, in general, complicated. For certain two-dimensional geometrical

arrangements, however, the creeping flow Stokes equation, modelling an incompressible liquid driven solely by surface tension, can be solved exactly using the technique of conformal mapping. One such an arrangement is the fibre-on-plate geometry where an infinitely long, isothermal cylinder is touching a flat plane at its periphery. The material is assumed to be a Newtonian viscous liquid with dynamic viscosity, η , density, ρ , and surface tension, γ . Let D_0 be the initial diameter of the cylinder. Using D_0 as the characteristic length and denoting the position variable by x_0 and the time by t_0 , the problem can be written in the dimensionless variables

$$x = \frac{X_0}{D_0} \quad (1a)$$

$$\tau = \frac{\gamma t_0}{\eta D_0} \quad (1b)$$

Hopper [1] showed that the evolution of shape with time is given exactly by the time-dependent mapping function

$$x(y) = \pm (y + a)(h/y - 1)^{1/2} \quad (2)$$

where $a = (1 - h^2)/4h$, $h = D/D_0$ and D is the actual cylinder height. Fig. 1 shows a plot of $x(y)$ for different values of h . This mapping represents the cylinder coalescing into half-space during time t .

Hopper further obtained the following relation between shape and time

$$\tau(\mu) = 2\pi \int_{\mu}^1 \frac{(2 - k^2)}{k^2(4 - 3k^2)^{3/2}(1 - k^2)^{1/2} K(k)} dk \quad (3)$$

with

$$\mu = 2h(1 + 3h^2)^{-1/2} \quad (4)$$

$$K(k) = \int_0^{\pi/2} (1 - k^2 \sin^2 \phi)^{-1/2} d\phi \quad (5)$$

* Also with Eindhoven University of Technology.

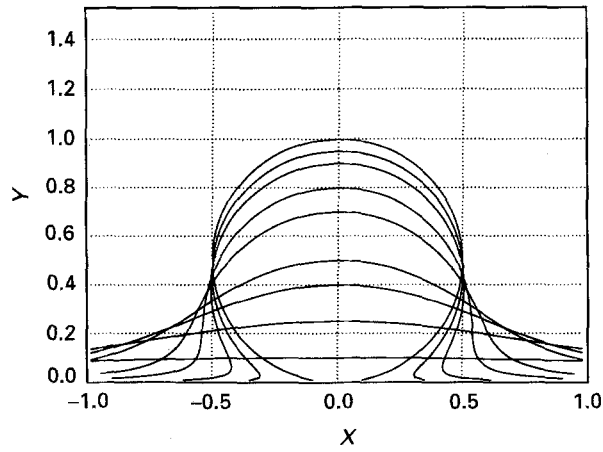


Figure 1 Map function for different values of h . The value of $y(0)$ represents h .

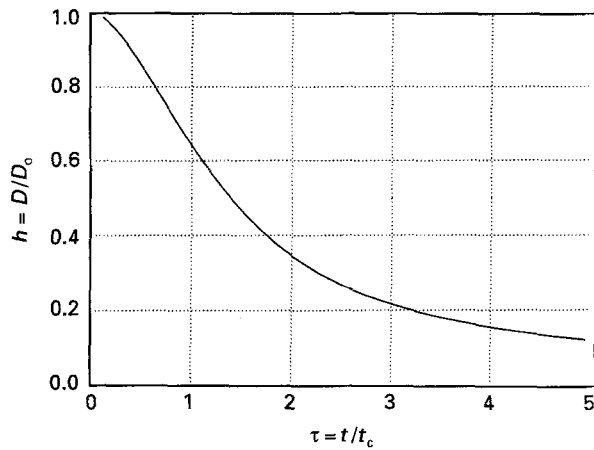


Figure 2 Dimensionless time, τ , versus dimensionless height, h .

The integral $K(k)$ is the complete elliptical integral of the first kind. Values of $K(k)$ can be obtained from the polynomial approximation [4]

$$K(k) = (a_0 + a_1 m + \dots + a_4 m^4) + (b_0 + b_1 m + \dots + b_4 m^4) \ln(m^{-1}) \quad (6)$$

with $m = 1 - k$, and

$$\begin{aligned} a_0 &= 1.386\ 294\ 361\ 12 & b_0 &= 0.5 \\ a_1 &= 0.096\ 663\ 442\ 59 & b_1 &= 0.124\ 985\ 935\ 97 \\ a_2 &= 0.035\ 900\ 923\ 83 & b_2 &= 0.068\ 802\ 485\ 76 \\ a_3 &= 0.037\ 425\ 637\ 13 & b_3 &= 0.033\ 283\ 553\ 46 \\ a_4 &= 0.014\ 511\ 962\ 12 & b_4 &= 0.004\ 417\ 870\ 12 \end{aligned}$$

Notice that for $k = 1$ the function $\tau(h)$ cannot be evaluated. Normal Simpson integration is not appropriate here. Therefore, $\tau(h)$ was computed by applying the Romberg integration [5]. Fig. 2 shows a graph of τ versus h .

In the course of this work, preprints of work by Korwin *et al.* [6, 7] were obtained in which the same theory was used for a study on the sintering behaviour of glass fibres. No attempts were made, however, to extract the surface tension from the experimental data.

3. Experimental procedure

All the samples used were sawn from one batch of modified Na–K–Ba–Sr–silica glass (63.5 SiO₂, 6.6 K₂O, 8.9 Na₂O, 8.1 BaO, 6.9 SrO, 3.5 Al₂O₃, 1.5 CaO, 1.0 remainder, wt %).

3.1. Viscosity

The viscosity of the glass was measured as a function of the temperature in a range of about 500–1500 °C [8]. Below 700 °C, the fibre extension method was used to determine the viscosity, while above 700 °C rotation viscometry was used. The viscosity data were determined for three batches of glass, produced at various times. Fitting these data with the Vogel–Fulcher–Tammann (VFT) equation [9]

$$\eta_{\text{VFT}}(T) = 10^{a+b/(T+c)} \quad (7)$$

using a Levenberg–Marquardt algorithm [5], resulted in the parameters given in Table I. Owing to relaxation processes, however, the viscosity of glass during heating or cooling is not only temperature-dependent but also time-dependent [9]. The relaxation function is frequently described with a sum of three exponentials [10]. Here the relaxation function is described by [11]:

$$E(t) = E_0 \sum_{i=1}^6 w_i e^{-t/\tau_i} \quad (8)$$

where w_i and τ_i denote the various weights and relaxation times, respectively. The parameter E_0 represents the unrelaxed modulus. The relaxation times can be determined at a certain reference temperature by a creep (retardation) experiment in a three point bending configuration. The retardation times thus obtained should be subsequently transformed to relaxation times [10, 11]. Since relaxation times for this particular glass are unknown, data for another glass with almost the same composition as the glass used were taken. These data, which are valid for a reference temperature of 493 °C, are given in Table II. The value of E_0 at the reference temperature was experimentally determined as 52 ± 3 GPa.

The viscosity at the reference temperature and infinite time can be calculated from

$$\eta(T_{\text{ref}}, \infty) = \frac{E_0}{3} \sum w_i \tau_i = \frac{E_0}{3} \bar{\tau} \quad (9)$$

Assuming that E_0 is constant with temperature, the relaxation time at temperature, T , can be calculated, assuming thermorheological simplicity [10], from

$$\tau_i(T) = \frac{\eta(T, \infty)}{\eta(T_{\text{ref}}, \infty)} \tau_{i,\text{ref}} \quad (10)$$

Having a sample at temperature T_1 with a (starting) viscosity pertaining to a temperature T_0 , the isothermal change of the viscosity is given by

$$\begin{aligned} \eta(t) &= \eta(T_1, \infty) + [\eta(T_0, \infty) \\ &\quad - \eta(T_1, \infty)] \sum w_i e^{-t/\tau_i} \end{aligned} \quad (11)$$

TABLE I Fit results of three series of viscosity data to $\log \eta = a + b/(T + c)$. The first value in a , b and c columns is for the fit to all data, the second for a fit to the fibre extension data only. The value in parentheses is the standard error. $\sigma^2(\text{fit}) = \sum |y_{\text{obs}} - y_{\text{calc}}|^2 / (n - m)$, with $y = \log \eta$

Batch	a	b	c	$\sigma(\text{fit})$	$\log \eta_{650^\circ\text{C}}$
1	-1.458 (0.12)	4408.99 (125)	-203.025 (6.58)	0.0806	8.406
	-4.103 (0.81)	6389.38 (709)	-135.073 (23.68)	0.0469	8.305
2	-1.568(0.081)	4522.22 (88)	-200.242 (4.58)	0.0552	8.487
	-3.877(0.618)	6323.38 (541)	-136.459 (18.33)	0.0363	8.436
3	-1.712(0.091)	4705.41 (100)	-189.239 (5.16)	0.0606	8.500
	-4.168(1.076)	6744.34 (981)	-116.688 (32.52)	0.0613	8.478
1 + 2 + 3	-1.582(0.062)	4547.81 (67)	-197.347 (3.49)	0.0725	8.465
	-4.063(0.777)	6497.48 (23)	-128.970 (23.02)	0.0776	8.408

TABLE II Relaxation times for a similar glass obtained from a creep experiment [11] at 493 °C

No.	Weight, W_i	Time, T_i (s)
1	0.0704	1.177
2	0.0964	11.19
3	0.2590	89.55
4	0.4596	515.0
5	0.1144	1692
6	0.0002	11916

In the non-isothermal case, the relaxation of the viscosity is more complex: temperature and relaxation times are dependent on time. At a certain time t_n , the relaxation of the viscosity will be given by the iterative equation

$$\eta(t_n, T_n, \tau_n) = \eta(T_n, \infty) + [\eta(T_{n-1}, t_{n-1}) - \eta(T_n, \infty)] \sum_i w_i e^{-(t_n - t_{n-1})/\tau_i(T_n)} \quad (12)$$

Fig. 3 shows the ageing effect. This was obtained by heating from 400 °C at a rate, dT/dt , of 0.1°C s^{-1} and taking as the starting viscosity, $\eta(T_0, \infty)$, the VFT viscosity at $T_0 = 480^\circ\text{C}$ (end temperature of the annealing procedure used, see below). It can be concluded from this graph that for a temperature $> 500^\circ\text{C}$ the mechanical ageing effect can be safely neglected. Slightly different values for T_0 and widely different values for dT/dt do not yield significantly different results.

This approach disregards structural relaxation. The structural relaxation behaviour is largely unknown. Increasing (decreasing) all relaxation times by a factor of 10 results in a coincidence temperature (Fig. 3) between the VFT viscosity and time-dependent viscosity of about 520°C (480°C). It is therefore very likely that all structural relaxation phenomena are insignificant above 525°C and the material therefore behaves in a purely viscous manner.

3.2. Annealing procedure

Residual thermal stresses in the glass, which could influence the relaxation experiments and result in damage to the samples during abrasive machining such as sawing and polishing, must be removed. Annealing is therefore required. The annealing process is

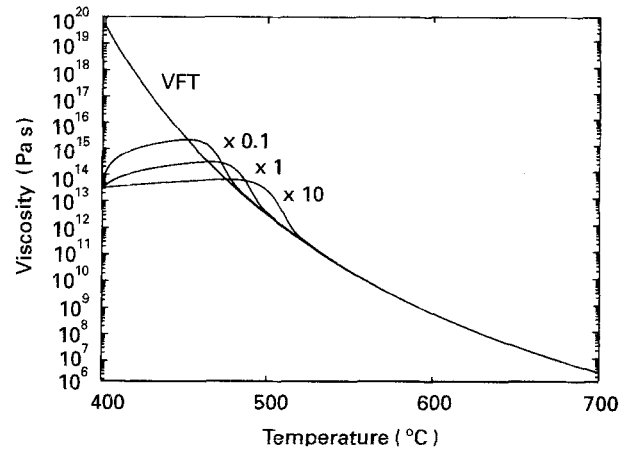


Figure 3 Ageing effect of viscosity. The continuously decreasing line is the viscosity as described by the time-independent VFT equation. The other lines labelled by the factors, denoting the multiplication factor for the as-measured relaxation times, represent the time-dependent viscosity-temperature behaviour. For details of the calculation, see text.

as follows: relaxation of stress at the annealing point for a certain time, slowly cooling down to the strain point, after which faster cooling down can be applied to reach room temperature. The annealing point and strain point of the glass are at 515°C and 480°C , respectively. For the 5 mm thick glass samples used, the following annealing procedure was always applied [12]: 480 min relaxation at 515°C , cooling at 12°C h^{-1} to 480°C and then at 350°C h^{-1} to 20°C . Determination of the residual stress with birefringence measurements (using an apparatus made available to us by F. de Leeuw) yielded a stress level of less than 0.3 MPa, in agreement with the level to be expected after the given thermal treatment.

3.3. Pre-baking

The physical contact between fibre and plate at the beginning of the experiments is not always ideal for relaxation experiments, so that the starting time for relaxation is uncertain. By pre-baking the fibre on the plate before the relaxation experiments, this problem can be avoided. Exact relaxation experiments are then carried out starting with already relaxed samples, for which the exact starting dimensions were determined. The initial dimensionless time, τ_p , was fixed from the

starting profile, as described in the next section. Pre-baking was carried out by heating up to 650 °C, holding for several minutes (dependent on fibre diameter), then cooling down to 515 °C, followed by the annealing procedure.

3.4. Height determination

For the determination of the height, various procedures were used. First the heat-treated specimens were cross-sectioned and polished. The height of the (relaxed) fibre on the plate was determined optically by microscope and mechanically by a stylus apparatus. With the optical method, a microscope with measuring ocular was used to determine the height of the relaxed fibre at both polished cross-sections. With the mechanical method the height of the relaxed fibre was determined by measuring the height of the sample at three points (right and left side of the fibre for base level and the height of the fibre itself) using a stylus with a flat top, 1 mm in diameter. The value of the relaxed fibre height, D , was calculated as $D = D' - (L + R)/2$, where D' is the as-measured height of the fibre and L and R denote the as-measured height of the base level at the left and right side of the fibre, respectively. At the position for the L and R measurements, the distance between the stylus and the central position of the fibre was about two fibre diameters. Three readings were taken for each sample and the results were averaged. The mechanical method is less time-consuming because it needs no laborious cross-sectioning and would be preferable if the results are accurate enough.

3.5. Shape parameter determination by mapping

After taking a photograph of both polished cross-sections of the test specimens (see Fig. 4 for some examples of cross-sections in various stages), the contours were recorded from the photographs by tracing them with a digitizer and stylus, connected to a computer. The traced contour and a contour generated for an estimated value of h were plotted simultaneously on a monitor. By adapting the value of h in such a way that a good visual match is observed, the best mapping shape parameter h was found (see Fig. 5 for some examples).

3.6. Experiments

Fibres of various diameters were drawn from a portion of glass cut from the same batch as mentioned above. Three pieces of fibre of the same diameter were positioned in parallel on a polished glass plate ($\sim 60 \times 30 \times 5$ mm). The diameter, D_0 , of the fibres near the six ends was determined by using a microscope. The sample was then pre-baked (see above), after which it was sawn into 12 samples ($\sim 15 \times 10 \times 5$ mm). In each sample a hole (diameter = 1 mm) was made through which a thermocouple could be led for temperature measurement. The depth of this hole below the glass surface was

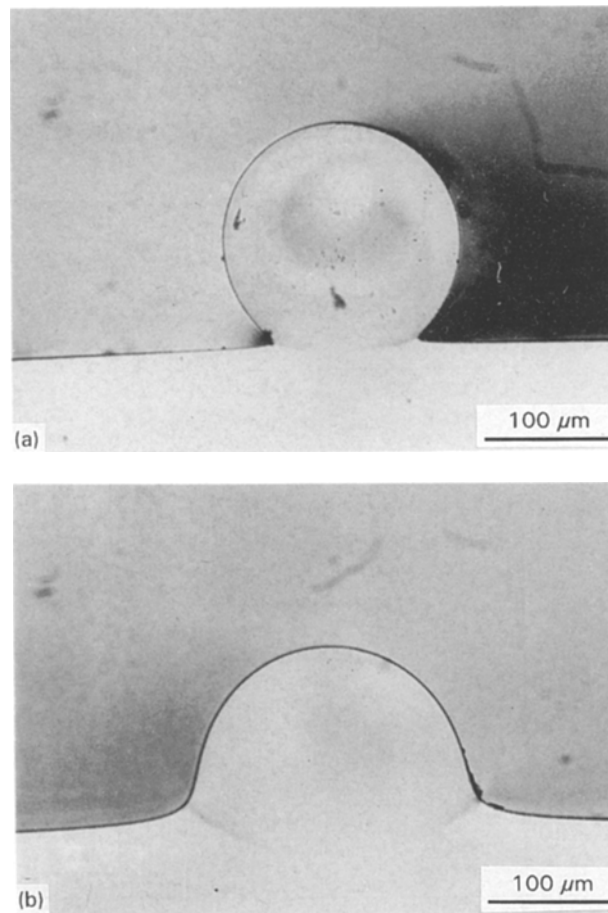


Figure 4 Example of photographs of (a) start and (b) final cross-sections of a sample.

approximately 1 mm. The samples were polished at both fibre cross-sections, after which the starting height, D_p , and shape were measured. The samples were subsequently relaxed at different temperatures and times by heating them at 350 °C h^{-1} to a certain top temperature, T_{top} , holding at T_{top} for Δt min, cooling at $\approx 1000 \text{ °C h}^{-1}$ to 515 °C, followed by the annealing process. After this the fibre cross-sections were sawn and polished again, and final height, D_r , and shape measurements were carried out. Examples of cross-sections at various stages are presented in Fig. 4.

The minimum size of fibre that can be handled without undue complications is about 50 μm . Accepting a measurement time of about 50 h results in a minimum experiment temperature of about 600 °C. Fibre diameters up to 200 and 1000 μm can be used with a contribution to the internal pressure due to gravity of less than 1% and 5%, respectively. Taking the latter diameter as the upper limit and allowing a minimum experiment time of 10 min to minimize heating and cooling effects, leads a maximum usable temperature of about 680 °C. This whole procedure was therefore applied to three sets of fibres with diameters of approximately 50, 130 and 190 μm (series I, II and III) while top temperatures used ranged from 600–680 °C and the time was varied between 10 and 3000 min.

During the experiments the temperature was computer-monitored and recorded using a Pt/Pt–10%Rh thermocouple. Readings were done with a calibrated

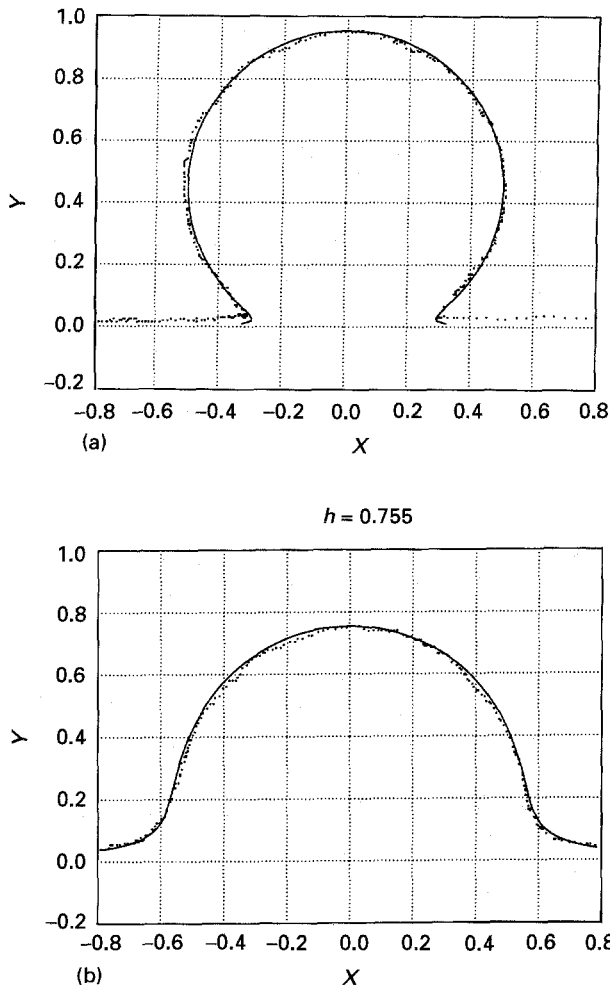


Figure 5 Traced profiles and map results of the (a) start ($h = 0.955$) and (b) final ($h = 0.755$) cross-sections shown in Fig. 4. The points are the traced data and the solid line is the best mapping profile retrieved.

thermometer (Fluke 2190A) gauged against a standard thermometer (Analogic AN6520).

4. Results and discussion

4.1. Relaxation of the shape

Fig. 4 shows an example of the cross-section of a fibre-on-plate in an initial stage and the corresponding final stage. The corresponding mappings are given in Fig. 5. There is excellent agreement between the shape obtained experimentally and the theoretical predictions of Hopper [1]. This is true for all experiments, the h -value ranging from 0.98–0.62. For the neck diameter a maximum relative difference of about 0.05 between the experimental and theoretical value was observed for $h \approx 0.95$. This indicates a somewhat better agreement than the corresponding value ranging from 0.10–0.15 as reported by Korwin [6]. In view of this agreement, an attempt was made to determine the surface tension of the glass from the relaxation profiles. The procedure followed is outlined below.

4.2. Surface tension determination

Because γ and η are temperature dependent and therefore not constant in time in our experiments, the

dimensionless time, τ , as given in Equation 1b, must be rewritten as

$$\tau = \int_0^r \gamma/\eta D_0 dt \quad (13)$$

Because of the pre-baking procedure used, the final dimensionless time, τ_r , is a result of the pre-baking ($t = 0 \rightarrow t_1$) and the procedure following it ($t = t_1 \rightarrow t_2$)

$$\tau_r = \int_0^{t_1} \gamma/\eta D_0 dt + \int_{t_1}^{t_2} \gamma/\eta D_0 dt \quad (14)$$

or

$$\tau_r = \tau_p + \int_{t_1}^{t_2} \gamma/\eta D_0 dt \quad (15)$$

The value of γ is only slightly dependent on temperature. The value of $d\gamma/dT$ was reported to be only -4×10^{-5} and $-5 \times 10^{-5} \text{ N m}^{-1} \text{ } ^\circ\text{C}^{-1}$ by Scholze [9] and Bondi [13] respectively. Taking γ constant with temperature and thus with time, we obtain

$$\gamma = (\tau_r - \tau_p) D_0 / \int_{t_1}^{t_2} 1/\eta dt \quad (16)$$

The same programmed temperatures resulted in almost the same measured top temperatures, despite all the intervening activities, which shows the reproducibility of the temperature measurements. For analysis of the data, the integrals $I_1 = \int 1/\eta dt$ and $I_2 = \int T/\eta dt$ are required and were calculated using the Romberg integration technique [5]. The effective temperature, T_{eff} , is calculated from $T_{\text{eff}} = I_2/I_1$. The viscosity at the effective temperature, $\eta(T_{\text{eff}})$, is calculated from the VFT equation using the parameters already mentioned. The values for the surface tension, γ , were calculated by using the “effective temperature” ($\gamma = \Delta\tau D_0 \eta(T_{\text{eff}})/\Delta t$) and also by using the “exact temperature” ($\gamma = \Delta\tau D_0/I_1$), for each of the applied height determination methods. The value of $\Delta\tau$ is calculated from $\Delta\tau = \tau_r - \tau_p$, with τ_r and τ_p being calculated from h_r and h_p , respectively. The effective temperature differed about 0.1 and 5°C for long and short top times, respectively, from the experimental top temperature. This resulted in a negligible difference in γ between the “effective temperature” and “exact temperature” method for long top times and up to a 50% difference in γ for short top times. The “exact temperature” method is considered to be the more reliable, because it takes all effects directly into account.

The averaged surface tension data obtained by optical, mechanical and mapping methods are given in Table III. The value found is typically about 0.19 N m^{-1} . Determination of the surface tension by the sessile drop method at approximately 1000°C resulted in a value of $0.336 \pm 0.007 \text{ N m}^{-1}$ [11]. Extrapolating to 650°C , using $d\gamma/dT = -4 \times 10^{-5} \text{ N m}^{-1} \text{ } ^\circ\text{C}^{-1}$ (after Scholze [9]), yields a value of 0.351 N m^{-1} . Comparing this value with the averaged values in Table III shows that it differs by a factor of approximately 1.75.

If a linear relation between γ and T is assumed, a similar procedure as described above can be applied.

TABLE III Mean surface tension data for separate series and series together using the “effective temperature” method (left) and the “exact temperature” method (right). The sample standard deviation, σ , is given in parentheses. $\sigma^2 = (\sum\gamma^2 - n\bar{\gamma}^2)/(n - 1)$

Series	n	$\gamma = \Delta\tau D_0 \eta / \Delta t$			$\gamma = \Delta\tau D_0 / l_1$		
		Opt.	Mech.	Map	Opt.	Mech.	Map
I	7	0.213 (0.061)	–	0.193 (0.062)	0.180 (0.024)	–	0.162 (0.040)
II	6	0.206 (0.059)	0.216 (0.072)	0.228 (0.027)	0.179 (0.031)	0.187 (0.034)	0.202 (0.015)
III	6	0.242 (0.090)	0.298 (0.131)	0.275 (0.126)	0.192 (0.062)	0.227 (0.078)	0.217 (0.097)
I + II + III		0.220 (0.069)	0.257 (0.11)	0.230 (0.084)	0.184 (0.040)	0.207 (0.061)	0.192 (0.062)

In view of the small value of $d\gamma/dT$, this would yield nearly identical results.

A generalized T -test can be used to assess the significance of the above-mentioned difference [14]. For convenience we represent the data as (mean, sample standard deviation, number of samples). For instance, compare the worst case, which is the one that differs least from the sessile-drop data. Table III shows that these are the data for the mechanical measurements using the “effective temperature” method. Comparing this value of $\gamma = (0.257, 0.11, 12) \text{ N m}^{-1}$ with the extrapolated value $\gamma = (0.351, 0.01, 3) \text{ N m}^{-1}$ yields a T -value of 2.91. Because the T -value for a significance level of 99% is 2.72, the difference can be considered as significant. The more reliable “exact temperature” method, again using the value from the mechanical measurements ($\gamma = (0.207, 0.061, 12) \text{ N m}^{-1}$) we have a T -value of 7.77, representing a significance level far above 99.9%.

4.3. Discussion of influencing factors

The following items are relevant for an analysis of the above-mentioned factor of 1.75 and they will be discussed in the next section:

1. mapping procedure to determine h ;
2. VFT fit parameters for viscosity;
3. temperature gradient in the furnace;
4. viscosity temperature sensitivity ($d\eta/dT$);
5. effect of atmosphere.

4.3.1. Mapping procedure

For three values of τ (0.3, 0.6 and 0.9), the relaxation profile was simulated with 0.5%, 1% and 2% Gaussian distributed noise upon the X and Y values. These nine shapes were plotted and, using the previously noted mapping procedure, the best-fitting shape parameter, h , was determined for each shape. See Fig. 6 for examples of simulated profiles and retrieved shapes. From these values for h , the dimensionless time, τ , was calculated. Experimental profiles contain a noise level of about 1%. Taking the same noise level for a simulated profile, it was shown that in that case a maximum error of 1% in $\Delta\tau$ can be expected using the mapping procedure. We conclude, therefore, that

measurement errors in τ for the mapping procedure cannot explain the difference between the fibre-on-plate value of $\gamma = 0.19 \text{ N m}^{-1}$ and the extrapolated sessile-drop value of 0.351 N m^{-1} . Because the other height determination methods yield comparable $\Delta\tau$ values, the same conclusion is also valid for these methods.

4.3.2. VFT fit

Let us review the VFT fit results as presented in Section 3. In Table I the fit results as obtained from the three sets of data are given. As can be seen, a rather good fit is obtained: the standard errors of the fit parameters are low and the standard fit error is small as compared with the $\log \eta$ data. Moreover, these data show that the quality of the glass as judged by the viscosity is essentially constant. For the purpose of further analysis the variation of the viscosity over batches is thus considered as negligible. Because the relaxation experiments were all carried out at a temperature below 700°C , the fit results of the separate fibre extension data are also listed. The standard fit error for the fibre extension data is somewhat lower than for the complete data. The values for the standard fit error vary from 0.080–0.036 and are low as compared with the $\log \eta$ values, varying from 1.9–14.5 dPa s. As can be seen, the fit parameters differ greatly, but the calculated value for $\log \eta_{650^\circ\text{C}}$ differs by a maximum of 2%. Actually, however, we use η instead of $\log \eta$ for the calculation of γ . A deviation of 2% in $\log \eta = 8.5$ represents a deviation in η of a factor $10^{8.5 \times 1.02} / 10^{8.5} = 1.48$. This means that the 2% variation in $\log \eta$ at 650°C , obtained by the various fits, can result in a 50% variation for the value of η . If we were to tolerate a maximum variation in η of 10%, the maximum variation in $\log \eta$ would be 0.5%. We conclude, therefore, that, although the consistency of the η data is excellent, the accuracy of the independent data is insufficient for an accurate estimate of γ .

4.3.3. Temperature gradient

Another factor may be the existence of a temperature gradient in the glass sample. To establish whether

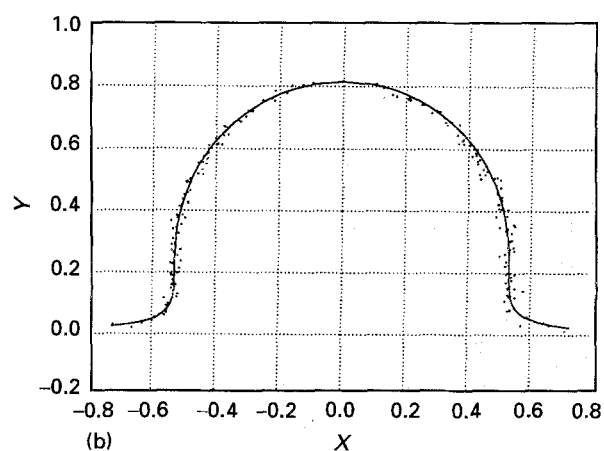
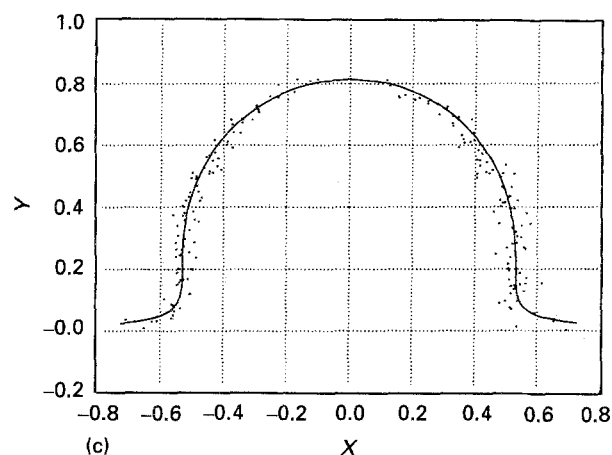
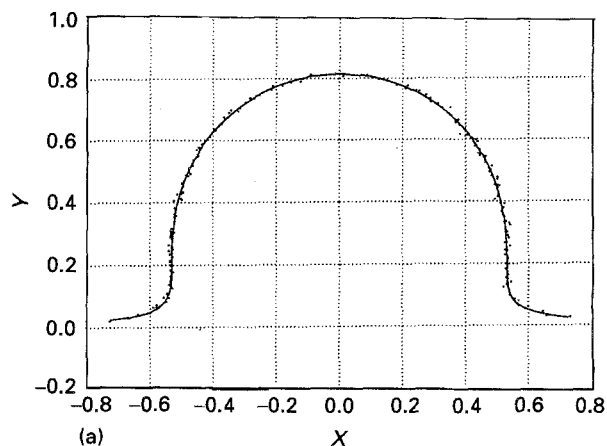


Figure 6 Simulated map functions for $\tau = 0.6$, $h = 0.815$ and noise levels of (a) 0.5%, (b) 1% and (c) 2%. Points are the simulated data, the line is the best mapping profile retrieved.

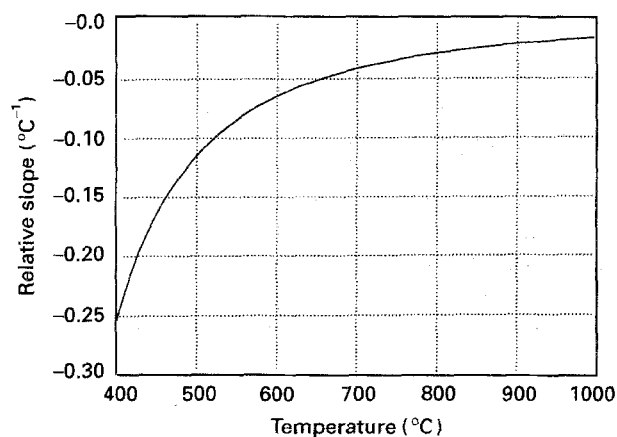


Figure 7 Relative slope of the viscosity versus the temperature.

such a temperature gradient existed in the height of the glass sample, we prepared a sample with three holes in it, positioned one above the other at 1 mm intervals. The top hole had the same depth below the glass surface as in the normal samples. A thermocouple was led through each hole and the sample was put into the furnace as already described (see Section 3). The sample was heated at 350°C h^{-1} to 450°C and the three thermocouples were read out after about 60 min stabilization. Subsequently readings were done at various temperatures, and also after ~ 60 min stabilization. The following sets of readings were obtained (upper, middle, lower hole): (468, 468, 468), (570, 570, 570), (618, 618, 618), (642, 643, 642), (667, 667, 667) and (693, 693, 692) $^\circ\text{C}$, at set points of 450, 550, 600, 625, 650 and 675°C , respectively. As can be seen, the temperatures are nearly the same. The lateral temperature gradient was also estimated by measuring the temperature at the centre and about 10 mm left and right from the centre at a depth of 1 mm. For the same set of temperatures mentioned above the corresponding readings were (left, centre, right): (476, 476, 475), (572, 572, 571), (622, 621, 620), (647, 646, 645), (672, 672, 670) and (696, 696, 695). Again the differences are negligible.

From these data we conclude that no temperature gradient existed and that the temperature was determined during the relaxation experiments to within 1°C . Finally, it should be mentioned that if the thermocouple is positioned about 1 cm below the surface of the specimen, a temperature difference of about

-10°C is obtained as compared with the measurement procedure as discussed here.

4.3.4. Viscosity-temperature sensitivity

The sensitivity of η as a function of temperature is obtained by determining the first derivative of the VFT equation. Taking the averaged parameters as noted in Section 3 we obtain a relative sensitivity $(d\eta/dT)/\eta$ versus T plot as shown in Fig. 7. Taking the absolute error in temperature during our experiments as about $\pm 1^\circ\text{C}$, results in a relative deviation in viscosity of $\pm 13\%$ at a relaxation temperature of 600°C , which means that the temperature sensitivity of the viscosity also contributes substantially to the inaccuracy in γ . However, it cannot explain the difference between the fibre-on-plate value and the extrapolated sessile-drop value.

4.3.5. Effect of atmosphere

Another possible explanation for the difference is the use of dry nitrogen gas for the sessile-drop experiments and air for the present measurements. The influence of the atmosphere is largely unknown, but it can be substantial at low temperature. At a temperature of about 1000°C the influence of water vapour on the

surface tension is negligible [15]. Let us focus on the low-temperature range. For instance, for silica glass [16] at room temperature the surface enthalpy for a silanol surface is 0.13 N m^{-1} , while for a siloxane surface the value amounts to 0.26 N m^{-1} . The reduction of surface energy of E-glass due to water-vapour adsorption was measured by Huang *et al.* [16] to be about 0.25 N m^{-1} at 20°C . For soda-lime silica glass Parikh [17] observed a decrease in surface tension, γ , at 550°C , varying from 0.315 N m^{-1} in a dry atmosphere to 0.205 N m^{-1} in a wet atmosphere. The water-vapour pressure used was about 21 mbar, which is about the saturation vapour pressure at room temperature. For 50% relative humidity (RH) the surface tension γ was about 0.230 N m^{-1} . In our case, too, air of about 50% RH was used, which makes it likely that a significant decrease in γ was present.

5. Conclusion

The first aim of this work was to verify experimentally the theoretical prediction of Hopper [1] for the fibre-on-plate geometry. Indeed the relaxation of the profile of the fibre-on-plate geometry is described very well by his model.

For the second aim, the applicability of the analysis for the determination of the surface tension of glass at low temperature, the following points hold. Given the viscosity as a function of temperature, the surface tension determined with this method yields $\gamma = 0.19 \text{ N m}^{-1}$ at 600°C for the glass studied. This value differs significantly from the extrapolated sessile drop value of 0.35 N m^{-1} . Possible origins of this difference are evaluated. The main factor is probably the difference in atmosphere, particularly the presence of water, which considerably lowers the surface tension at low temperature. Furthermore, we conclude that the accuracy of the viscosity data and the temperature sensitivity of the viscosity are the most important limiting factors for obtaining an accurate γ value. This means that very accurate temperature readings and very accurate VFT parameters are necessary for accurate γ determinations. Mechanical measurements of the height by a stylus apparatus seem adequate, however, thus offering the possibility of avoiding elaborate cross-sectioning. Moreover, it is shown that in the case of this glass, viscosity ageing effects are probably negligible above about 525°C .

The fibre-on-plate method relies on the dynamics of a deformation process, while the sessile-drop method relies only on the equilibrium profile. Consequently, the former method is inherently inferior. This explains the greater inaccuracy. In view of the temperature sensitivity and high dependency on the viscosity data, it is probably better to measure the surface tension and viscosity at low temperature, together but independently, in a fibre extension experiment.

Acknowledgements

The authors thank Mr H. van Dam for making available to us the viscosity data, Mr F. de Leeuw for the residual stress measurements, Dr J. v. d. Brink for the relaxation and surface tension data, and Mr W. Horden for cross-sectioning and polishing the specimens.

References

1. R. W. HOPPER, *J. Fluid Mech.* **243** (1992) 171.
2. H. K. KUIKEN, *Coll. Surf.* **59** (1991) 129.
3. S. B. G. M. O'BRIEN, *J. Adhes. Sci. Technol.* **6** (1992) 1037.
4. M. ABROMOWITZ and I. A. STEGUN, "Handbook of Mathematical Functions" (Dover, New York, 1972).
5. W. H. PRESS, B. P. FLANNERY, S. A. TEUKOLSKY and W. T. VETTERLING, "Numerical Recipes in Pascal" (Cambridge University Press, Cambridge, 1990).
6. D. M. KORWIN, S. R. LANGE, W. C. EATON, I. JOSEPH and L. D. PYE, in "Proceedings of 16th Int. Congress on Glass 9", Madrid edited by A. Durán and J. M. F. Navaro, Vol. 2, (Int. Com. Glass, Madrid, 1992) p. 253.
7. D. M. KORWIN, W. C. EATON and L. D. PYE, *J. Am. Ceram. Soc.* submitted.
8. H. B. B. VAN DAM, personal communication (1993).
9. H. SCHOLZE, "Glas: Natur, Struktur und Eigenschaften", 2nd Edn (Springer, Berlin, 1977).
10. G. W. SCHERER, "Relaxation in Glass and Composites" (Wiley, New York, 1986).
11. J. v. d. BRINK, personal communication (1993).
12. G. W. MOREY, "The Properties of Glass" (Reinhold, New York, 1954).
13. A. BONDI, *Chem. Rev.* **52** (1953) 417.
14. J. R. GREEN and D. MARGERISON, "Statistical Treatment of Experimental Data" (Elsevier, Amsterdam, 1978).
15. R. K. ILLER, "The Chemistry of Silica" (Wiley, New York, 1975) p. 645.
16. R. J. HUANG, T. DEMIREL and T. D. MCGEE, *J. Am. Ceram. Soc.* **56** (1973) 87.
17. N. M. PARIKH, *ibid.* **41** (1958) 18.

Received 2 February
and accepted 4 October 1994